

Precipitation Effects in Diffused Transistor Structures

J. M. Fairfield and G. H. Schwuttke

Citation: *Journal of Applied Physics* **37**, 1536 (1966); doi: 10.1063/1.1708563

View online: <http://dx.doi.org/10.1063/1.1708563>

View Table of Contents: <http://scitation.aip.org/content/aip/journal/jap/37/4?ver=pdfcov>

Published by the [AIP Publishing](#)

Articles you may be interested in

[Phosphorus diffusion effect on defect structure of silicon with oxygen precipitates revealed by gold diffusion study](#)

Appl. Phys. Lett. **67**, 2054 (1995); 10.1063/1.115076

[Effect of oxygen precipitation on phosphorus diffusion in Czochralski silicon](#)

Appl. Phys. Lett. **53**, 34 (1988); 10.1063/1.100114

[Diffusion and precipitation in amorphous Si](#)

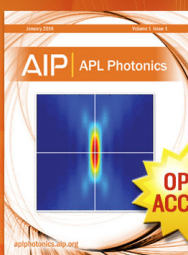
Appl. Phys. Lett. **46**, 478 (1985); 10.1063/1.95563

[The effects of impurity diffusion and surface damage on oxygen precipitation in silicon](#)

J. Appl. Phys. **54**, 388 (1983); 10.1063/1.331714

[Effect of concentration-dependent diffusion coefficients on precipitate growth kinetics](#)

J. Appl. Phys. **43**, 4443 (1972); 10.1063/1.1660941



Launching in 2016!

The future of applied photonics research is here

AIP | APL
Photonics

Precipitation Effects in Diffused Transistor Structures*

J. M. FAIRFIELD AND G. H. SCHWUTTKE

International Business Machines Corporation, East Fishkill, New York

(Received 25 October 1965)

Transmission x-ray diffraction microscopy was used to detect precipitation effects in phosphorus-diffused silicon—especially after subsequent gold diffusion. The precipitate (after gold diffusion) appears to be a complex—formed by gold combining with excess phosphorus in the silicon lattice. This complex formation is responsible for the apparent high solubility of gold in phosphorus-diffused areas, and it has a potentially detrimental effect upon diode reverse characteristics. Furthermore, this phenomenon provides a sink for gold atoms that would otherwise fill silicon lattice sites. This effect has important consequences on the fabrication of fast switching devices, since it tends to rob the crystal lattice of gold recombination centers.

INTRODUCTION

RECENTLY it has been reported¹⁻³ that phosphorus-diffused layers (N^+) retard gold diffusion into silicon and increase its solubility, whereas boron-diffused layers (P^+) do not retard gold diffusion. Since gold is used quite extensively to control storage times of silicon devices, it is important to understand the conditions under which excess gold collects in N^+ areas, and the nature of the gold once it is there. Although it is not known why gold increases in solubility in phosphorus-doped areas, Wilcox *et al.*¹ have proposed two mechanisms to explain this phenomenon, to wit: the interaction of gold atoms with an enhanced vacancy concentration in the N^+ area or a compound formation involving gold and phosphorus.

To date, little has been reported about either the physical nature of this excess gold or its effects upon crystal perfection and device performance. This paper reports an investigation to understand more fully the conditions under which excess gold collects in N^+ areas. It correlates crystal imperfection patterns and gold concentration for various types of diffused areas. It presents x-ray evidence for the suggested mechanism of compound formation and also shows the effects of this compound upon such diode characteristics as recovery time and reverse breakdown voltage.

EXPERIMENTAL PROCEDURE

Planar phosphorus-diffused structures were fabricated by means of standard⁴ open-tube diffusion and SiO_2 masking techniques. Also for comparison, planar boron- and arsenic-diffused structures were similarly^{5,6} made. The characteristics of the diffusions are summarized in Table I. Junction depths were typically 1μ .

* Sponsored in part under Contract AF19(628)-5059.

¹ W. R. Wilcox, T. J. LaChapelle, and D. H. Forbes, *J. Electrochem. Soc.* **111**, 1377 (1964).

² E. Kooi, *J. Electrochem. Soc.* **111**, 1383 (1964).

³ J. W. Adamic, Jr., and J. E. McNamara, Washington Meeting of Electrochemical Society, October 1964, Abstract No. 153.

⁴ R. P. Donovan and A. M. Smith, New York Meeting of Electrochemical Society, October 1963, Abstract No. 150.

⁵ M. C. Duffy, O. R. Viva, and W. J. Armstrong, San Francisco Meeting of Electrochemical Society, May 1965, Abstract No. 125.

⁶ W. J. Armstrong and M. C. Duffy, *Electrochem. Tech.* (to be published).

For gold diffusion, pure gold was evaporated onto the back of the silicon wafers and diffused at $1000^\circ C$ in a nitrogen atmosphere. Normally a diffusion time of two hours was used; however, for one phase of the investigation, the gold diffusion time was varied in order to study its effect upon diode recovery time. The total gold concentrations were determined by standard radiotracer or activation techniques. In some cases, the gold diffusant was tagged with $Au-199$ and analyzed in a manner described earlier.⁷ For activation analysis, wafers containing gold, along with control wafers without gold, were irradiated in a thermal neutron flux of about 10^{13} n/cm²-sec. (Ref. 8) for a few days and similarly analyzed.

Large-area x-ray topographs were made to study crystal imperfection patterns of the planar diffused regions before and after gold diffusion. The x-ray topographs were recorded through the use of SOT.⁹

In addition, we examined the diode storage times and reverse characteristics of these diffused structures, and have thus gained an understanding of the nature of gold in the silicon lattice and its effects upon diode behavior. From diode storage times (taken at forward-to-reverse current ratio of 1), we calculated the concentration of

TABLE I. Characteristics of the diffusions.

Diode type	Diffusant & method	Source	Surface concentration (C_0)
P^+N	Boron open tube	$B_2H_6^a$	$\sim 4 \times 10^{20}$ cm ⁻³
P^+N	Boron sealed tube	B-Si alloy ^b	10^{20} cm ⁻³
N^+P	Arsenic sealed tube	As-Si alloy ^b	2×10^{20} cm ⁻³
N^+P	Phosphorus open tube	P_2O_5	$> 10^{21}$ cm ⁻³
N^+P	Phosphorus open tube	PH_3	2×10^{20} to 2×10^{21} cm ⁻³

^a Ref. 5.

^b Ref. 6.

⁷ G. J. Sprokel and J. M. Fairfield, *J. Electrochem. Soc.* **112**, 200 (1965).

⁸ Union Carbide Corp., Nuclear Division, Tuxedo, New York.

⁹ G. H. Schwuttke, *J. Appl. Phys.* **36**, 2712 (1965).

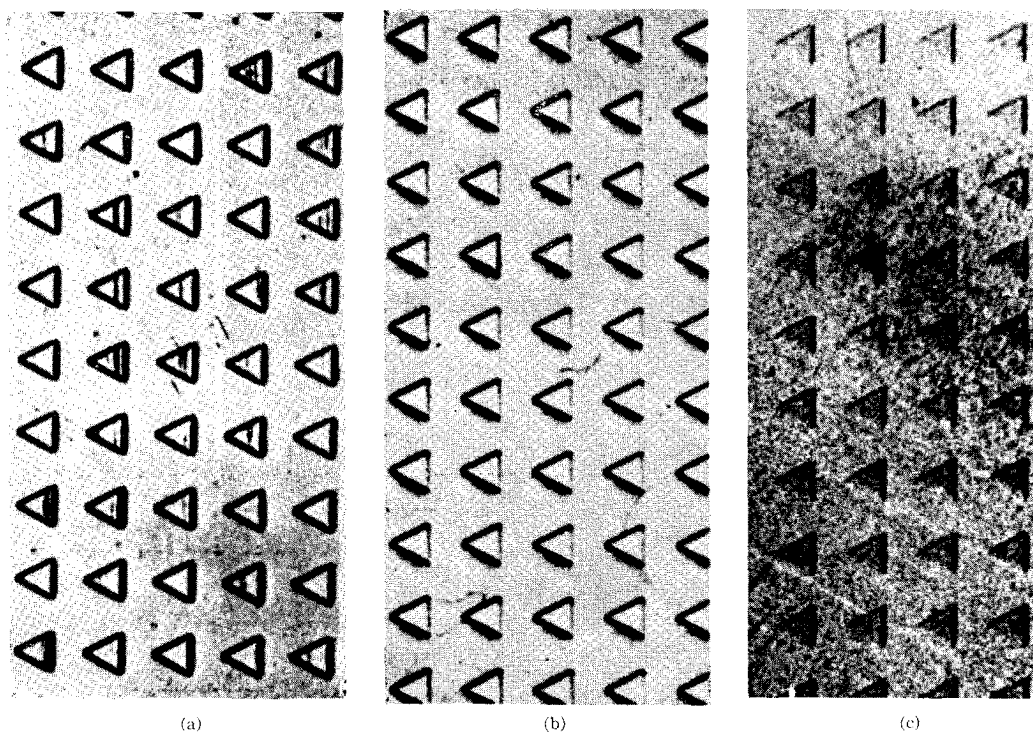


FIG. 1. X-ray topographs of diffused silicon wafers: (a) boron diffused, conc. $\approx 5 \times 10^{20} \text{ cm}^{-3}$; (b) phosphorus diffused, conc. $= 2 \times 10^{20} \text{ cm}^{-3}$; (c) phosphorus diffused, conc. $= 2 \times 10^{21} \text{ cm}^{-3}$.

gold recombination centers, generally assumed to be the gold in the substitutional lattice sites in or near the diffused areas. (The recombination model, necessary for this calculation, as well as the empirical justification, has been described in an earlier report.¹⁰) The reverse characteristics were measured using a diffused guard ring (of the type described by Coetzberger *et al.*¹¹) to suppress surface breakdown. We established a reverse criterion¹² and measured silicon wafer yields before and after gold diffusion. We also recorded some reverse I - V plots and examined the light emission of typical diodes in avalanche.

RESULTS AND DISCUSSION

X-ray topographs of these diffused structures show unique diffraction features; therefore, imperfection patterns in devices introduced through device processing can be detected and analyzed.⁹ Essentially, one has to differentiate between two distinct diffraction effects: (a) excess diffraction intensity along the boundary line silicon oxide-silicon (which coincides with the location of the junction); and/or (b) excess diffraction intensity inside the device area. Effect (a) is realized in Figs. 1

and 2 (triangular device structure) and in Fig. 3 (circular device structure). The contrast of the boundary line silicon oxide-silicon is strongly reflection-dependent. This is seen in Figs. 1, 2, and 3 for the triangular as well as for the circular device structures. Whenever a boundary line (or part of it) is perpendicular to the diffracting plane, it does not produce diffraction contrast.⁹ The condition of zero contrast is fulfilled for two sides of the triangle in Fig. 2(a), and for the hypotenuses in Fig. 2(b). It is almost fulfilled for one triangle side in Fig. 1(b); therefore, this side produces less contrast than the other two. In Fig. 1(a), the diffraction conditions are such that all three sides are visible with good contrast. If the device structure is circular, one part of its boundary line is always perpendicular to the diffracting plane—independent of the operating reflection. Consequently, the diffraction image of a circular device is two half-circles [Figs. 3(a), (b)].

The other striking diffraction effect caused by diffused junction structures is shown in Fig. 1(c). Comparing the areas inside and outside of the triangles and of the circles, it is evident that the diffused area diffracts considerably more intensity—this area is more faulted than the rest of the crystal. A faulted device area such as seen in Figs. 1(c), 2, and 3 is typical for a phosphorus diffusion. The degree of faulting can be correlated with the surface concentration. If the surface concentration is less than $4 \times 10^{20} \text{ cm}^{-3}$, no excess diffraction contrast

¹⁰ J. M. Fairfield and B. V. Gokhale, *Solid State Electron.* **8**, 685 (1965).

¹¹ A. Goetzberger, B. McDonald, R. H. Haitz, and R. M. Scarlett, *J. Appl. Phys.* **34**, 1591 (1963).

¹² Reverse criterion: A diode is considered "good" if the low current breakdown ($20 \mu\text{A}$) is within 15% of true avalanche.

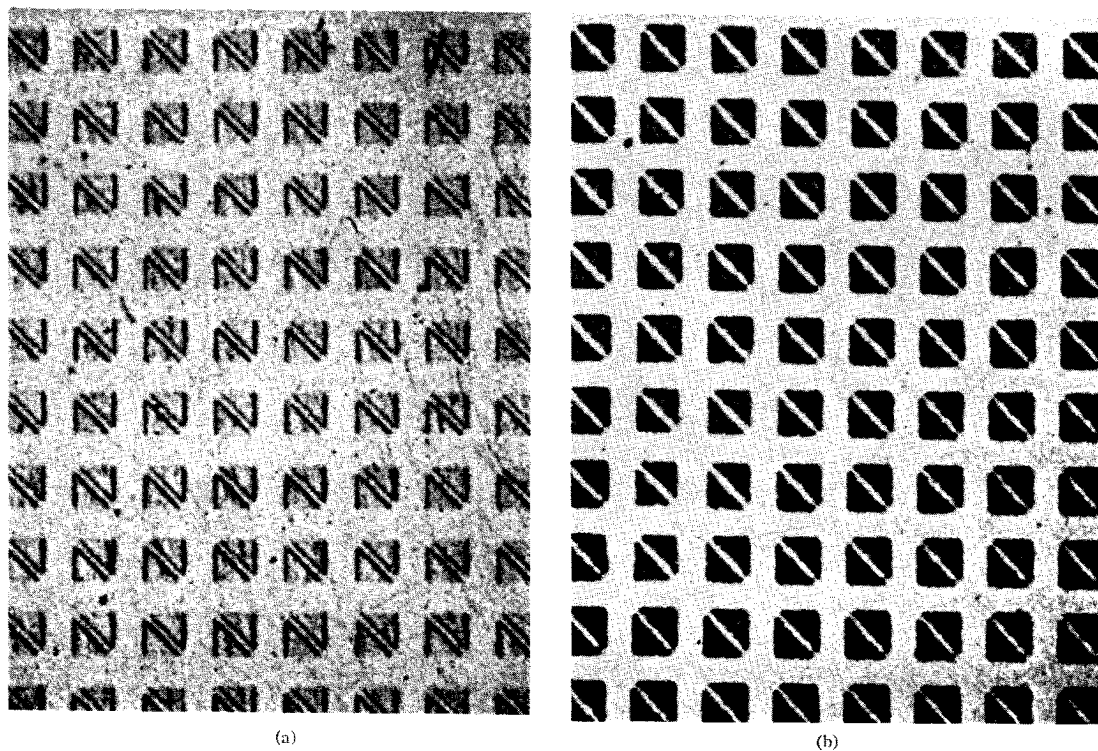


FIG. 2. X-ray topographs of phosphorus-diffused wafers, conc. = 10^{21} : (a) before gold diffusion; (b) after gold diffusion.

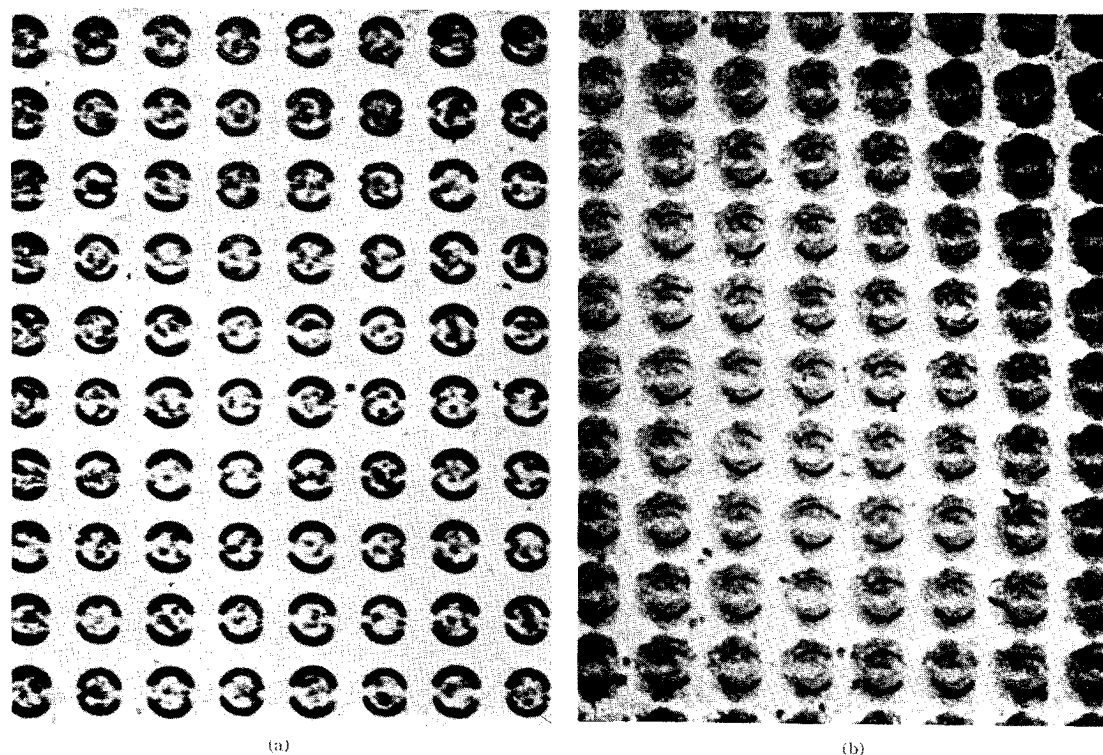


FIG. 3. X-ray topographs of phosphorus-diffused wafers after gold diffusion:
(a) conc. = $1 \times 10^{21} \text{ cm}^{-3}$; (b) conc. = $2 \times 10^{21} \text{ cm}^{-3}$.

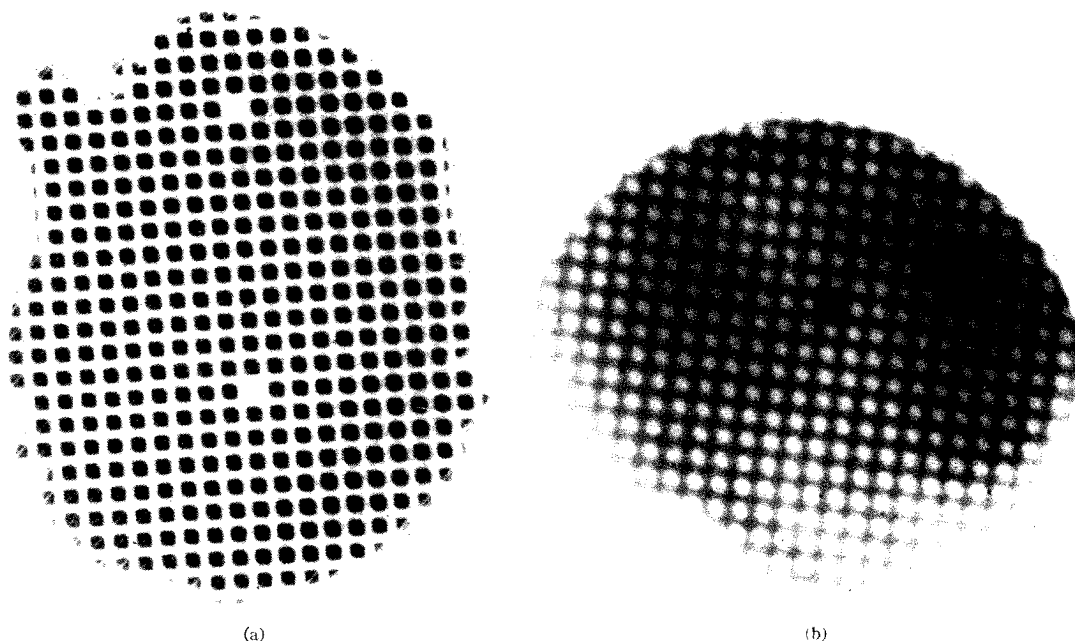


Fig. 4. Autoradiograms of wafer shown in Fig. 2; dark areas indicate larger gold concentration; (a) after gold diffusion, (b) after gold diffusion and removal of 3μ from top surface.

is found inside the device area [Fig. 1(b)]. For a surface concentration larger than 10^{21} cm^{-3} , the device area diffracts more intensity than the rest of the crystal.

In these topographs, the contrast in the diffused areas can be either uniformly dark [Fig. 1(c)] or become localized at certain points and very strong [Figs. 2(a) and 3(a)]. Uniform darkening is indicative of a high dislocation density (larger than $10^7/\text{cm}^2$) in the device area. Phosphorus diffusion introduces dislocations into silicon when the surface concentration exceeds 10^{21} cm^{-3} (Ref. 13). Dislocation densities as high as 10^9 cm^{-2} after phosphorus diffusion have been reported for standard open-tube diffusion.¹⁴ Our x-ray results indicate that defects induced through localized diffusion are confined to the device area. Diffusion-induced dislocations lie in the diffusion plane¹³; consequently, dislocations must bend upwards toward the Si surface in the direct vicinity of the diffusion window edges. The question whether the dislocations bend upwards and penetrate the silicon surface underneath the oxide or whether they come up at the exact position of the silicon oxide-silicon edge cannot be decided from our x-ray measurements.

After phosphorus diffusion, it is found many times that the diffraction contrast in the device area is not uniform, but is localized and very strong at certain points. Diffraction effects of this kind [Figs. 2(a), 3(a)] are due to the presence of precipitates in the device area. The x-ray results shown in Figs. 2(a) and 3(a)

indicate that the device contains either one or a few relatively large (larger than 1μ) precipitates or clusters. The parameters controlling the occurrence of such clusters are presently not understood. However, cluster formation is typical for phosphorus diffusion and is favored in the presence of oxygen.

A device area after boron diffusion (surface concentration $\leq 5 \times 10^{20} \text{ cm}^{-3}$) does not show excess diffraction intensity. For very high surface concentrations ($5 \times 10^{20} \text{ cm}^{-3}$), dislocations of the Lomer-Cottrell type have been found in the device area. An example is shown in Fig. 1(a); there, the device area contains lines in $[110]$ and $[\bar{1}\bar{1}0]$ direction. The topograph in Fig. 1(a) was recorded through a 220 reflection; therefore, dislocation lines in $[110]$ are not visible (Burgers vector lying in the reflecting plane), whereas the $[\bar{1}\bar{1}0]$ lines appear with maximum contrast (Burgers vector perpendicular to the reflecting planes). For the 220 topograph (not shown), the situation is reversed.

An additional striking difference between diffraction contrast of boron- and phosphorus-diffused areas has been observed after a subsequent gold diffusion. For all boron surface concentrations and low-phosphorus surface concentrations, x-ray topographs look identical before and after gold diffusion. (This is also true if the first diffusion is arsenic.) However, whenever the x-ray topograph reveals excess diffraction contrast in the device area after phosphorus diffusion, a subsequent gold diffusion produces *additional* excess diffraction contrast (Fig. 2). This additional contrast is interpreted as heavy precipitation of a second phase and is in agreement with transmission electron microscopy

¹³ G. H. Schwuttke and H. J. Queisser, J. Appl. Phys. **33**, 1540 (1962).

¹⁴ J. L. Joshi and F. Wilhelm, J. Electrochem. Soc. **112**, 185 (1965).

TABLE II. Gold diffusion; 2 h at 1000°C.

Diode description	Minority carrier lifetime ^a (nsec)	Base material doping (cm ⁻³)	Gold recombination center density ^a (cm ⁻³)	Estimate of total gold (radiotracer) (cm ⁻³)
Boron diffusion	$\tau_p = 5.4$	$N_D = 4 \times 10^{16}$	10^{16}	10^{16}
Arsenic diffusion	$\tau_n = 7.4$	$P_D = 10^{17}$	6×10^{15}	$3-8 \times 10^{15}$
Low-concentration phosphorus diffusion (4×10^{20} cm ⁻³)	$\tau_n = 11.0$	$P_D = 10^{17}$	4×10^{15}	$3-8 \times 10^{15}$
High-concentration phosphorus diffusion (2×10^{21} cm ⁻³)	$\tau_n = 40.0$	$P_D = 10^{17}$	10^{15}	$> 10^{17}$

^a Calculated from diode storage times (Ref. 10).

results.¹⁵ Radiotracer experiments have shown that this excessive precipitation involves gold.⁷ Figure 4(a) shows an autoradiogram of the wafer, whose imperfection pattern is illustrated in Fig. 2. The dark areas show the heavy gold concentration—found to be greater than 10^{17} cm⁻³ for gold diffusion times of 2 h (1000°C). This value is one order of magnitude larger than the solid solubility of gold in the silicon lattice for this diffusion temperature.¹⁶ The pattern in Fig. 4(a) persists to depths equal to or even a few microns greater than the electrical junction depth—after which the pattern reverses [Fig. 4(b)], indicating that the surrounding crystal lattice is depleted of gold. This phenomenon is similar to that reported previously.^{3,7} The radiotracer experiments did not show excessive gold concentrations in areas diffused with boron, arsenic, or low-concentration phosphorus, in good agreement with the x-ray results. Thus, the precipitated second phase is interpreted to be a P-Au type of complex. It should be noted that these experiments do not exclude the possibility of other elements being involved, e.g., oxygen or silicon.

The formation of this complex was found to have a significant effect upon the switching properties of these diffused junctions. Diode storage times were measured for diodes (prepared as described above) and compared with total gold concentrations taken from the radiotracer data. The results are shown in Table II, where it can be seen that, for diodes of high-concentration phosphorus, only a small amount of the total gold exists substitutionally in the lattice sites, i.e., as recombination centers. The remaining gold must exist as a part of the precipitated second phase. For all other diodes, most of the gold exists in the substitutional sites. In order to pursue this phenomenon further, we have studied the relationship of diode recovery to gold diffusion time at 1000°C for the arsenic and phosphorus diodes. The results are shown in Fig. 5, in which the reciprocal of minority carrier lifetime (calculated from diode storage time), as well as the calculated recombination center density, is plotted against diffusion time for the three types of N⁺P diodes. For diodes of high-concentration phosphorus, the rate of increase of gold recombination centers is relatively slow, due to the formation of the second phase complex. These diodes require diffusion times in excess of 30 h to reach saturation. For diodes of lower-concentration phosphorus (4×10^{20}),

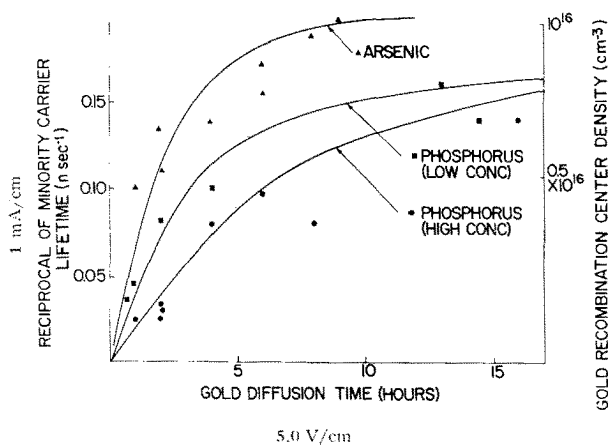


FIG. 5. Minority carrier lifetime or gold recombination center density vs gold diffusion time for arsenic (Δ), for low-conc. phosphorus (\blacksquare), and for high-conc. phosphorus (\bullet) diffused diodes.

¹⁵ F. Wilhelm and M. L. Joshi, IBM, Poughkeepsie (private communication).

¹⁶ C. B. Collins, R. O. Carlson, and C. J. Gallagher, Phys. Rev. **105**, 1168 (1957).

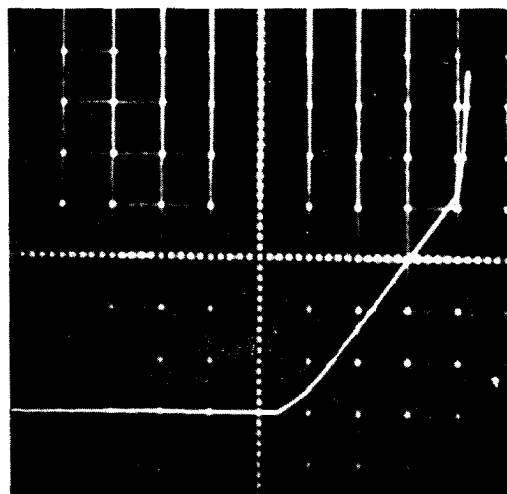


FIG. 6. I/V plot of a gold-doped phosphorus diode, indicating double break characteristic.

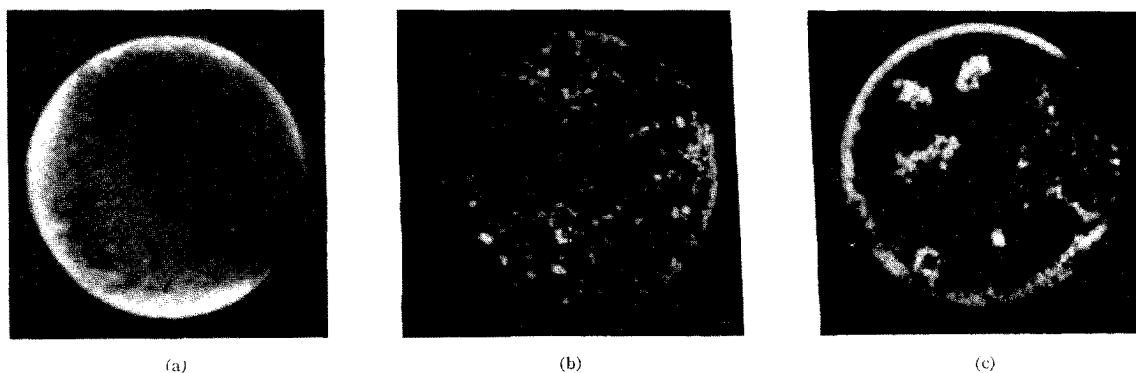


FIG. 7. Light emission patterns of phosphorus-diffused diodes in breakdown (avalanche breakdown = 50 V): (a) no gold; (b) gold-doped, low-current breakdown = 42 V; (c) gold-doped, low-current breakdown = 32 V (similar to I/V plot of Fig. 6).

this effect is less—but still present; recombination centers accumulate faster than for diodes of high-concentration phosphorus, but slower than for arsenic diodes. For arsenic diodes, gold recombination centers accumulate at the fastest rate of the N^+P diodes. Thus, the formation of the second phase provides a sink that inhibits the accumulation of gold recombination centers (of gold atoms in the silicon lattice sites). We assume that this process is responsible for the apparent high concentration of gold in N^+ silicon. This is a very important consideration in designing fast-switching transistors.

Finally, the precipitated second phase had relatively little effect upon the true avalanche breakdown (≈ 50 V)—but it decreased the low-current breakdown ($20 \mu A$) by amounts of up to 30%. A “good diode” yield of 90% is typical for wafers before gold diffusion; and yields of from 40% up to almost 90% (depending upon the degree of precipitation) are typical after gold diffusion. (Fig. 3, discussed above, shows the imperfection patterns of diodes used in this phase of the investigation.) This phenomenon can be associated with localized avalanche breakdowns at specific points within the diode area, similar in nature to the mechanism discussed by Shockley for localized breakdowns around SiO_2 particles.¹⁷ The $I-V$ plots of the poorer diodes indicated a “double break” characteristic and, at voltages between the apparent low-level breakdown and true avalanche, the current was limited by a series resistance of 10^3 to $10^4 \Omega$ —consistent with the spreading resistance expected for small current sources in a $p-n$

junction.¹⁷ (Original wafer resistivity was about $1 \Omega \cdot cm$.) An $I-V$ plot is shown in Fig. 6 for one of the poorest diodes. The gold did not cause a serious degree of junction “softness”; that is, a “rounding” effect of the $I-V$ plot. However, we did not investigate extremely low-current levels or high ambient temperatures.

The light emission patterns of two typical diodes in breakdown are shown in Fig. 7, along with one before-gold-diffusion for comparison. The diode pictured in the center shows many small microplasmas randomly located. The diode on the right also shows the small microplasmas but clustered at certain places which correspond to points of high precipitation. These points of high precipitation are shown in Fig. 3 by the strong localized contrast. This last diode showed maximum effects from the precipitation.

It should be pointed out that much of this effect of gold upon the reverse characteristics may not be noticed if the diffused guard ring is not used, since the breakdown at the surface was often less than the localized avalanche breakdowns due to precipitation.

ACKNOWLEDGMENTS

The authors are indebted to Tom Hansen and C. Hoogendoorn for their help in performing the x-ray work, and to R. Racicot for the diffusion work.

Part of the work was sponsored by the Air Force Cambridge Research Labs., Office of Aerospace Research, U. S. Air Force, Bedford, Mass., under Contract No. AF19(628)-5059.

¹⁷ W. Shockley, *Solid-State Electron.* **2**, 35 (1961).